The Journal of Veterinary Medical Science

FULL PAPER

Pathology

Immunohistochemical detection of virus antigen in the nasal planum of rabid dogs

Chun-Ho PARK[1)]*, Sayaka KUBONIWA[1)], Ryo MURAKAMI[1)], Nozomi SHIWA[2)], Satoshi INOUE[1,3)], Kazunori KIMITSUKI[4)], Ma. Ricci R. GOMEZ[5)], Mark Joseph M. ESPINO[5)], Alpha Grace B. CABIC[5)], Sheila Marie C. ESPOSO[5)] and Daria L. MANALO[5)]

[1)]Department of Veterinary Pathology, School of Veterinary Medicine, Kitasato University, 23-35-1 Higashi, Towada, Aomori 034-8628, Japan
[2)]National Institute of Infectious Diseases, Gakuen 4-7-1, Musashimurayama-shi, Tokyo 208-0011, Japan
[3)]National Institute of Infectious Diseases, Toyama 1-23-1, Shinjuku-ku, Tokyo 162-8640 Japan
[4)]Department of Microbiology, Faculty of Medicine, Oita University, Yufu, Oita 879-5593 Japan
[5)]Research Institute for Tropical Medicine, Muntinlupa City 1781, Philippines

ABSTRACT. The rabies virus is one of the most neurotropic of all viruses infecting mammals. During the terminal phases of infection, the virus spreads to peripheral tissues, including the skin. The external skin of the nose, called the nasal planum, is a sensory organ where numerous nerve bundles and terminal nerves are distributed. Therefore, the nasal planum is expected to serve as a postmortem diagnostic material. However, the distribution of rabies virus antigens in the nasal planum in rabid animals has not yet been studied. In this study, the nasal planum was obtained from 45 rabid dogs. In all rabid dogs, the viral antigen was detected in the peripheral nerve tissues, Merkel cells, and squamous cells. The viral antigen in the epidermis exhibited three patterns: first, a diffuse positive pattern from the basal layer to the squamous layer; second, a reticular positive pattern along the cell membrane in the squamous layer; and third, a basal layer pattern of the epidermis. In the dermis, viral antigens were detected more often in lamellated corpuscles just beneath the rete pegs. These results suggest that the nasal planum could serve as a useful alternative source for postmortem diagnosis in rabies endemic countries.

KEY WORDS: dog rabies, immunohistochemistry, nasal planum skin, postmortem diagnosis

J. Vet. Med. Sci.
83(10): 1563–1569, 2021
doi: 10.1292/jvms.21-0438

Received: 5 August 2021
Accepted: 24 August 2021
Advanced Epub:
2 September 2021

Rabies is a highly fatal zoonotic disease transmitted to humans through bites from infected animals, and causes acute encephalomyelitis after a variable incubation period. In Asian countries, domestic dogs are the primary sources of rabies, and a majority of human rabies deaths are associated with dog bites [7]. The direct fluorescent antibody test (DFAT) is the gold standard for rabies diagnosis [26, 27] and is a highly sensitive and quick method for detecting rabies antigens in fresh specimens. However, the sensitivity of DFAT and immunoperoxidase methods is reduced under unsuitable postmortem conditions, such as warm temperatures [2, 16]. Underreporting of dead rabid animals in the field is also very common. The sampling and transport of brain specimens from a local area to a diagnostic laboratory can be laborious, causing delays. Therefore, the identification and characterization of alternative types of specimens for the postmortem diagnosis of canine rabies via low-cost, simple tests associated with a low risk of viral exposure are required in rabies-endemic countries.

We previously reported that follicle-sinus complexes (FSCs; also known as whiskers or vibrissae) in the facial skin are useful specimens for rabies diagnosis, not only in domestic animals [21, 24] but also in wild animals [23]. In FSCs, viral antigens were detected in a part of the outer root sheath at the level of the ring sinus of FSCs of the facial skin, and a majority of the cells were positive for Merkel cell (MC) markers, with viral particles observed in the MC cytoplasm. MCs are known as specialized cutaneous receptor cells and are located at high concentrations not only in facial haired skin but also in glabrous skin, such as nasal skin, principally glabrous nasal skin, and lips in dogs [20]. In addition, it is also known that glabrous nasal skin is innervated by a branch of the trigeminal nerve and that nerve endings are densely distributed in the dermis and epidermis in dogs [1, 18, 25]. These morphological features suggest that glabrous nasal skin may be useful as an alternative postmortem diagnostic source for rabid dogs, considering that the rabies virus shows strong neurotropism. To our knowledge, there are no published studies that have examined the distribution of viral antigens in the glabrous nasal skin of rabid animals. In this study, we investigated the pattern of viral antigen distribution in the glabrous nasal skin (nasal planum) of rabid dogs.

*Correspondence to: Park, C.-H.: baku@vmas.kitasato-u.ac.jp

MATERIALS AND METHODS

Animals

Nasal planum samples were obtained from 45 rabid dogs and submitted to the Research Institute for Tropical Medicine (RITM) of the Philippines for postmortem diagnosis of rabies. Twenty-eight dogs were found dead, whereas 17 were euthanized. The age of 45 dogs (19 males, 15 females, and 11 of unknown sex) ranged from 1 month to more than 15 years, and that of 9 dogs was unknown. None of the dogs had a history of rabies vaccination. The primary clinical symptoms of canine rabies infection, such as unprovoked aggressiveness, mad biting of inanimate objects, aimless running, and excessive salivation were observed in 25 of the 45 dogs, and no information was available for the remaining dogs. All dogs tested positive for rabies virus antigen in the hippocampus via the DFAT.

Histopathological examination

Nasal planum samples were fixed in 10% neutral buffered formalin solution for at least 72 hr and trimmed such that the transversal aspect of the nose was sectioned. Transverse sections (5 mm thick) of the nose were cut at the level of the alar fold, excess tissue was trimmed off, and the right nasal planum (Fig. 1) was submitted for histopathological and immunohistochemical analyses. Paraffin-embedded blocks, sectioned at 3 μm thickness, were stained with hematoxylin and eosin (HE) or by the immunohistochemical methods described below. Samples from three beagle dogs used in other experiments, aged 10 months, vaccinated against rabies were used as negative controls.

Immunohistochemistry (IHC)

To avoid misjudgment between the viral antigen-positive staining and melanin pigments, all tissue sections were bleached with 20% hydrogen peroxide for 15 hr at room temperature (RT) before IHC. For detection of the rabies viral antigen in tissues, sections were stained using a streptavidin–biotin–peroxidase complex method with rabbit anti-phosphoprotein (P), as described previously [6]. The following primary antibodies were used to detect the cell type: mouse anti-cytokeratin 20 (CK 20, Nichirei Biosciences, Tokyo, Japan) as a marker of MCs [17, 19] and mouse anti-neurofilament protein (NF, Dako, Kyoto, Japan) as a marker of nerve fibers. Briefly, for the activation of antigens, tissue sections were treated with 0.25% trypsin at RT for 30 min for anti-P antibodies, microwaved at 170 W for 10 min for CK 20, and treated with proteinase K for 15 min for NF. To remove endogenous peroxidase, the sections were treated with 3% H_2O_2 in methanol. To block nonspecific reactions, sections were treated with 10% normal goat or rabbit serum. Primary antibodies were diluted 1:1,000 (anti-P) in PBS and incubated at 4°C overnight in a humidified chamber. Anti-rabbit IgG (Nichirei Biosciences) was used as the secondary antibody for anti-P. The Envision + System Labeled Polymer-HRP anti-mouse antibody (DAKO) was used as a secondary antibody for CK20, and Histofine Simple Stain MAX-PO anti-mouse (Nichirei Biosciences) was used for NF. Antibodies were visualized using 3-3′-diaminobenzidine (DAKO). Finally, the slides were counterstained with hematoxylin.

Double immunofluorescence staining

To identify cell types that expressed the viral antigens, double staining of a single tissue section was conducted using the immunofluorescent antibody technique [21]. To evaluate the relationship between viral antigen-positive cells and MCs, combined staining with anti-P and CK 20 antibodies was done. To block nonspecific reactions, sections were treated with 10% normal goat serum. The primary antibodies were diluted as described above. FITC-conjugated goat anti-rabbit IgG (H+L) (Southern Biotechnology Associates, Inc., Birmingham, AL, USA) and Alexa Fluor 546-conjugated goat anti-mouse IgG (H+L) (Thermo Fisher Scientific, Inc., Waltham, MA, USA) were used as secondary antibodies at 1:200 dilutions. DAPI (Thermo Fisher Scientific) was used for counterstaining.

Transmission electron microscopy

Transmission electron microscopy was performed to observe viral particles in MCs, squamous cells, and nerve tissue. Nasal planum tissues embedded in paraffin wax were cut into 1 mm blocks, deparaffinized, and dehydrated in an ethanol series. The tissue pieces were washed with PBS, post-fixed for 12 hr at RT in 1% buffered osmium tetroxide, and embedded in epoxy resin. Approximately 70 nm-thick sections were stained with uranyl acetate and lead citrate and examined using a transmission electron microscope (H-7650, Hitachi, Tokyo, Japan).

RESULTS

Histopathological and immunohistochemical findings in the nasal planum from control and rabid dogs

We first investigated the morphological structure of the nasal planum from control dogs and compared the differences with that from the rabid dogs. All control dogs had defined epithelial domes, which were composed of one cornified layer, squamous layer up to about 30 layers, and a basal layer (Fig. 2). The squamous layer extended toward the dermis, and elongated dermal papillae protruded into the epidermal layer. Melanin pigments were observed throughout all layers of the epidermis and were highly concentrated in the basal layer. The dermis was mainly composed of collagen bundles, blood vessels, and nerve bundles. Nerve bundles were larger in the deeper layers of the dermis than in the superficial layers. Nerve bundles in the superficial layers of the dermis lacked myelin structures and often formed encapsulated lamellated corpuscles of various sizes up to 30 μm (Fig. 3). NF-

positive findings were confirmed in the nerve bundles (Fig. 4) and lamellated corpuscles (Fig. 5) in the dermis. In the epidermis, some of the thin nerve fibers extended toward the squamous epithelial layer, and a majority of the nerve fibers ended in the deep layers of the epidermis (Fig. 4). CK 20 staining gave positive results, suggesting that MCs were clustered at the basal areas of the rete pegs (Fig. 6).

In rabid dogs, focal to multifocal necrosis and cytolysis of the epithelial cells were localized in the basal and deep squamous layers of the rete pegs (Fig. 7) in 10 of the 45 dogs. In these cases, mild infiltration of lymphocytes, plasma cells, and macrophages was observed in the superficial layers of the dermis and perivascular areas. However, pathological changes were not observed in the cornified layer or dermal nerve tissue. Cytoplasmic eosinophilic inclusion bodies, called Negri bodies, were not observed in any component of the nasal planum skin.

Viral antigens were detected in the epidermis and dermis of the nasal planum (Fig. 8A) in all rabid dogs. The distribution of the positive staining for viral antigens varied and exhibited three main patterns: first, a diffuse positive pattern from the basal layer to the squamous layer (Fig. 8B); second, a reticular positive pattern along the cell membrane in the squamous layer (Fig. 8C); and third, a basal layer pattern of the epidermis (Fig. 8D). All the three patterns were observed for each sample. Among the strong positive patterns in the basal layer of the rete pegs, a majority of the cells were positive for both anti-P and CK 20 (Fig. 9). In 10 rabid dogs, in the squamous epithelial cells that showed necrosis and cytolysis, the viral antigen-positive reaction was weak compared with that in the other intact squamous epithelial cells, and was absent in some cases. Viral antigens were rarely found in

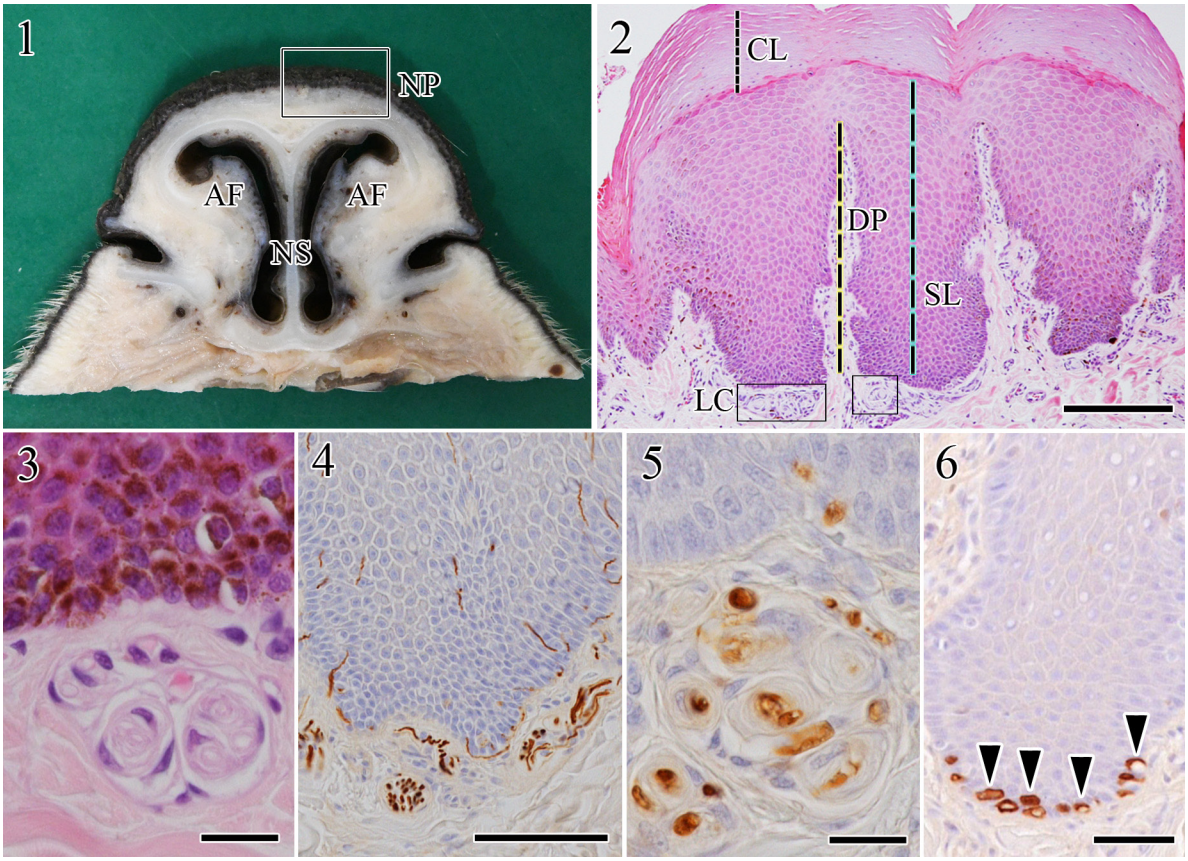

Fig. 1. Gross findings of the nasal planum. The nasal planum was cut at the position of the alar fold. In transverse sections, the top boxed area indicates right nasal planum examined in this study. AF: alar fold, NP: nasal planum, NS: nasal septum.

Fig. 2. Normal morphological features of the nasal planum. Epidermal dome composed of a cornified layer (CL), squamous layer (SL), dermal papillae (DP), and lamellated corpuscles (LC, solid line). Hematoxylin eosin staining, bar=200 µm.

Fig. 3. Lamellated corpuscles of various sizes, immediately below the epidermis. Unmyelinated nerve fibers surrounded by Schwann-like cells. Hematoxylin eosin staining, bar=20 µm.

Fig. 4. Immunohistochemical images of nasal planum section labeled with a neurofilament antibody. Numerous nerve bundles in dermis and free nerve endings invading the epidermis are seen. Immunohistochemistry, bar=100 µm.

Fig. 5. Immunohistochemical images of lamellated corpuscles. The centers of the lamellated corpuscles are strongly positive for the neurofilament antibody, but Schwann-like cells and their process are negatively stained. Immunohistochemistry, bar=20 µm.

Fig. 6. Immunohistochemical images of the rete pegs in the epidermis. CK 20-positive Merkel cells (arrowheads) are clustered in the basal areas of the rete pegs. Immunohistochemistry, bar=50 µm.

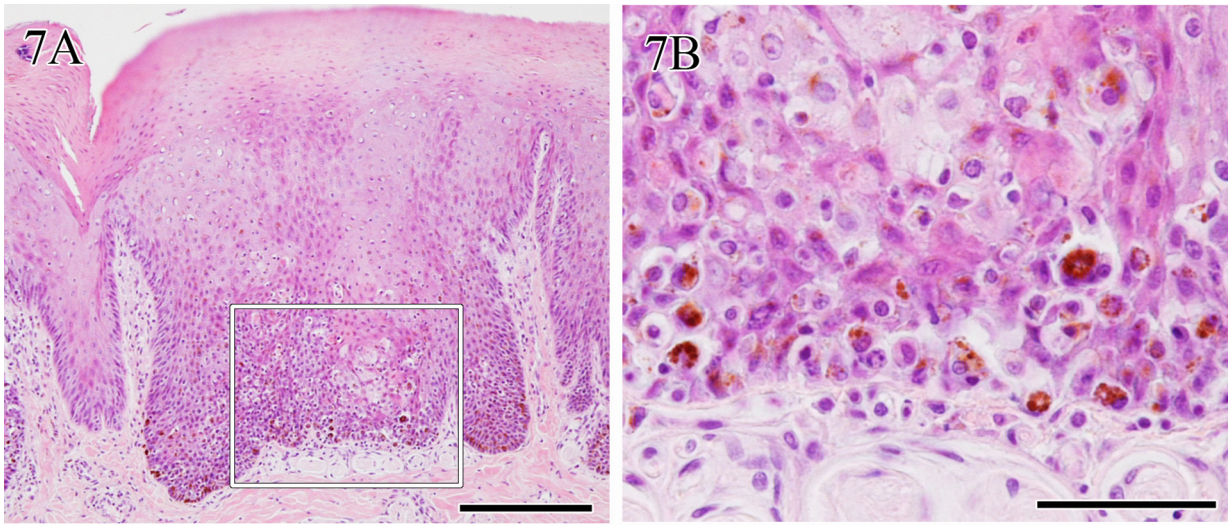

Fig. 7. A focal inflammatory lesion in the rete pegs in the epidermis (boxed area). An enlarged image of the boxed area shows necrosis and lysis of epithelial cells in the basal layer. Hematoxylin eosin staining, bar=200 µm (A) and 50 µm (B).

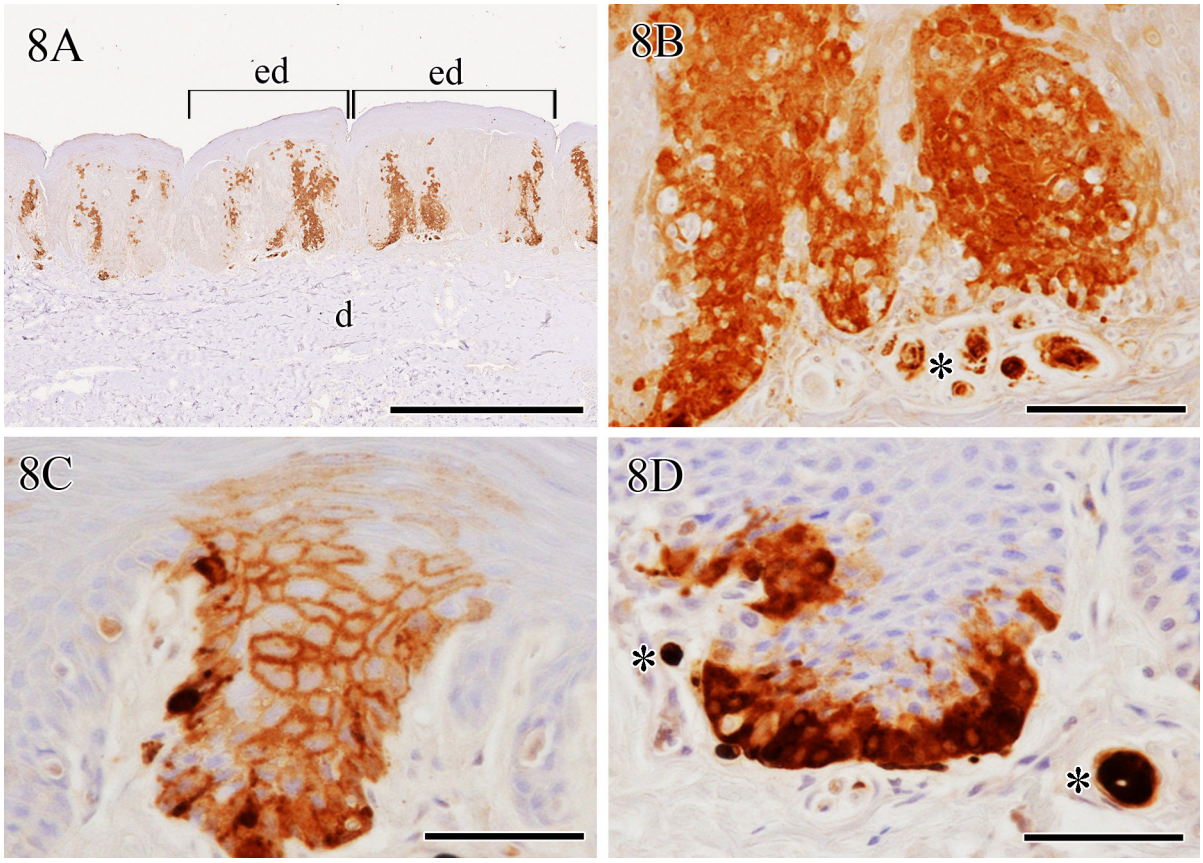

Fig. 8. The distribution of the positive staining for viral antigen varied from small focal areas to extensive staining of a majority of the epithelial cells **(A)**. At higher magnification, diffuse positive **(B)**, reticular **(C)**, and strong positive **(D)** patterns in the basal layer of epidermis are seen. In addition, strong positive staining in the lamellated corpuscles (asterisks in B, D) immediately beneath the epidermal rete pegs is seen. d: dermis, ed: epidermal dome. Immunohistochemistry, bar=1 mm (A), 100 µm (B), 50 µm (C, D).

the cornified layers of the epidermis. In the dermis, viral antigens were found more often in the lamellated corpuscles just beneath the rete pegs, and showed strong intensity compared with large nerve bundles located in the deeper layers of the dermis.

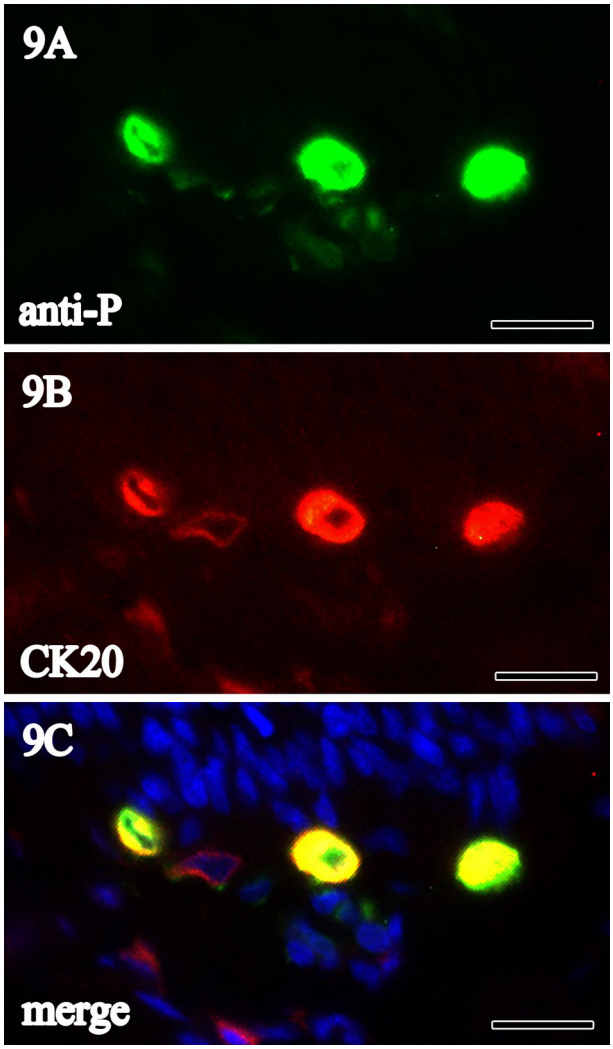

Fig. 9. Immunofluorescence staining images for viral antigen (**A**, anti-P, green) and CK 20 (**B**, red), and double-positive signals (**C**, merged images, yellow), in the basal layer of the epidermis. bar=20 µm.

Ultrastructural findings

Viral particles (approximately 150 nm long and 70 nm wide) were observed in the rough endoplasmic reticulum of squamous cells (Fig. 10A, 10B), MC nerve endings, and lamellated corpuscles. Virus-associated circular-to-tubular structures within or near the endoplasmic reticulum and small ill-defined granular matrix (approximately 500–1,000 nm in width) were rarely observed in the cytoplasm of squamous cells (Fig. 10C), MC nerve endings (Fig. 10D, 10F), and lamellated corpuscles.

DISCUSSION

The aim of this study was to describe the localization of viral antigens in the nasal planum of rabid dogs and to evaluate their diagnostic utility in identifying rabies. Using light microscopy, histopathological lesions including necrosis and cytolysis were found in the basal layer of the epidermis in 10 of the 45 dogs examined and viral antigen was detected. These pathological findings were similar to those reported by us previously, showing that the rabies virus replicated and caused varying degrees of necrosis of the squamous cells in the FSCs of rabid dogs [21]. It is unknown why these pathological lesions were mainly localized in the basal layer of the epidermis, or whether they were directly induced by viral infection in the epithelial cells. However, they might have resulted from differences in the density of innervation, the quantity of virus replication among the basal and superficial layers of epidermis, individual differences in the stages of infection, or the limited area of the nasal skin used for examination.

In rabies, the most characteristic histopathological findings are intracytoplasmic inclusion bodies called Negri bodies [13]. In general, inclusions are considered products of the infectious process, and matrix inclusions become larger with time, making them detectable in hematoxylin and eosin-stained sections by light microscopy. Lahaye *et al*. discovered through *in vitro* experiments that Negri bodies are sites of viral transcription and replication, and contain viral RNA, N and P proteins, heat shock protein Hsp70, Toll-like receptor 3, and ubiquitinylated proteins [14]. In animal and human rabies, inclusions tend to occur more frequently in large neurons, such as the pyramidal neurons of the hippocampus and cerebral cortex, neurons of the medulla oblongata, and Purkinje cells of the cerebellum [11, 12]. In this study, inclusions were not found in the epithelial cells of the epidermis or peripheral nerve tissue in the dermis of the nasal planum by light microscopic observation. In addition, the matrix size was small, and viral particles and virus-associated structures were rarely found in the squamous cells, MCs, or lamellated corpuscles upon ultrastructural observation. These results were similar to those of previously reported studies on non-neuronal tissues, such as salivary gland acinar cells [6, 22] and epithelial cells in the skin [9]. Therefore, it was suggested that the viral infection in the nasal planum was delayed compared with that in the central nervous system, and the dog died or was euthanized before larger inclusions were formed in the nasal planum. However, because the mechanism underlying the morphogenesis and functional characterization of the Negri body in the infected cells is still not well understood [10, 14, 15], the exact nature of this association requires further investigation.

In this study, viral antigens were detected in epithelial cells of the epidermis and peripheral nerve tissue in the dermis. In neuroanatomy, the external nasal nerve is a terminal branch of the trigeminal nerve [8]. Trigeminal nerve branches into three nerves, one of which is the ophthalmic nerve, with three branches, one of which is the nasociliary nerve. One of the terminal branches of the nasociliary nerve is the anterior ethmoidal nerve, which divides into the lateral nasal branch and the medial nasal branch. After giving off sensory branches to the anterior and upper parts of the nasal septum, the medial nasal branch emerges from beneath the inferior nasal margin to form the external nasal nerve. The external nasal nerve provides sensory innervation to the skin of the external nose. In dogs, the nasal planum skin is densely packed with sensory fibers. Some nerve fibers terminate at the lamellated corpuscles in the superficial dermis or MCs, and fine unmyelinated nerve fibers penetrate through the basement membrane and appear in the intercellular spaces of the epidermis [1, 25]. Therefore, it is concluded that the unique antigen-positive pattern and variation in intensity observed in this study may depend on the differences in innervation or density of the terminal

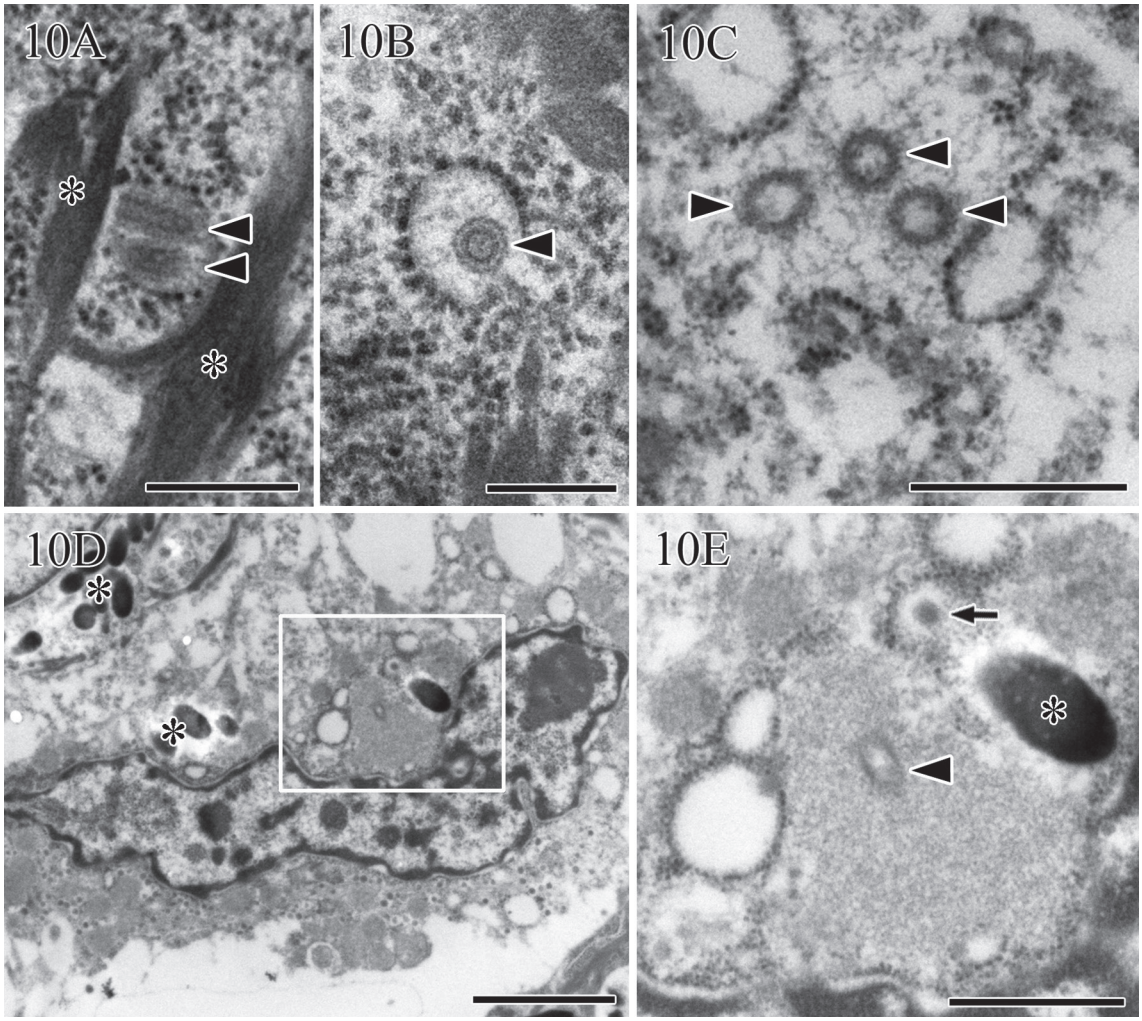

Fig. 10. Virus particles are observed in the longitudinal (arrowheads, **A**) and transverse (arrowhead, **B**) images of the endoplasmic reticulum of squamous cells. Virus-associated circular structures (arrowheads, **C**) are observed in the matrix in the cytoplasm of squamous cells. Matrix structures are seen in the cytoplasm of Merkel cells (boxed area, **D**). At higher magnification of the boxed area, virus-associated tubular structures (arrowhead, **E**) and viral particles (arrow, **E**) in the endoplasmic reticulum are seen. Asterisks (*) indicate keratin filament (A) and melanin granules (D, E). Transmission electron microscopy, bar=300 nm (A), 200 nm (B), 500 nm (C), 2 µm (D), 500 nm (E).

nerve endings. However, the possibility of direct cell-to-cell transmission of virus without using free nerve endings in the epidermis cannot be ruled out. Further studies are needed to examine this.

During the terminal phases of infection, the rabies virus disseminates centrifugally to peripheral tissues, and viral antigens can be detected by immunohistochemistry or immunofluorescence examination of the peripheral nerves in epidermal cells of the skin and hair follicles [3–5]. In animals and humans, skin biopsies, including hair follicles, are used for intra vitam or postmortem diagnosis [11, 12]. The proportion of positive results increases as the disease progresses. We previously reported that FSCs in the facial skin of dogs are optimal as postmortem diagnostic material because they are surrounded by numerous nerve fibers and have a high density of Merkel nerve endings, which are targets for virus replication [21]. In this study, MCs were located in the rete pegs of the epidermal dome as clusters, and a majority of the MCs were positive for the virus antigen, and virus particles were found. Therefore, it was reconfirmed that MCs are targets of viral infection. Forty-two of the 45 dogs in this study were used in a previous study employing FSCs [24]. There was no difference in the antigen-positivity rate between FSCs and nasal planum. Therefore, it was concluded that both these tissues are useful as alternative sources for the diagnosis of rabies in dogs. However, we believe that the use of nasal planum is more advantageous than that of FSCs because the sampling of nasal planum is easier than that of FSCs and it can be easily cut at the same level of the alar fold.

In summary, the pathological findings of this study indicate that rabies virus descends centrifugally in the nasal planum using trigeminal nerve branches, and the virus replicates in the sensory corpuscle, MCs, intraepithelial nerve endings, and squamous epithelial cells. Although the intensity of antigen positivity varied from case to case, the amount of viral antigen was sufficient to be detected by light microscopy in all cases. These results reflect that innervation density in nasal planum skin was deeply associated with virus dissemination and infection phases in dogs submitted to this study, which were in late or terminal phases of

illness. Sampling the nasal planum skin is easier and safer than sampling brain tissue. Thus, nasal planum skin may be useful not only as an alternative postmortem source for the diagnosis of rabies, but also for epidemiological studies on both domestic and wild animals.

CONFLICT OF INTEREST. The authors declare no conflict of interest in the present study.

ACKNOWLEDGMENTS. The authors would like to acknowledge the invaluable help of staff at the Research Institute for Tropical Medicine (RITM) Department of Health and Regional Animal Disease Diagnostic Laboratory III (RADDL III) for tissue collection from dogs in the current study. This work was supported by a Grant-in-Aid for Scientific Research from the Japan Society for the Promotion of Science (Kakenhi No. 26450410), and a grant for scientific research from the KITASATO University, Heiwa Nakajima Foundation, and JICA/AMED, SATREPS (Science and Technology Research Partnership for Sustainable Development), Japan.

REFERENCES

1. Abe, Y. 1954. Fine structure of nasal and oral cavities in dog and their sensory innervation, especially on the intraepithelial fibres. *Tohoku J. Exp. Med.* **60**: 115–128. [Medline] [CrossRef]
2. Arslan, A., Saglam, Y. S. and Temur, A. 2004. Detection of rabies viral antigens in non-autolysed and autolysed tissues by using an immunoperoxidase technique. *Vet. Rec.* **155**: 550–552. [Medline] [CrossRef]
3. Balachandran, A. and Charlton, K. 1994. Experimental rabies infection of non-nervous tissues in skunks (*Mephitis mephitis*) and foxes (*Vulpes vulpes*). *Vet. Pathol.* **31**: 93–102. [Medline] [CrossRef]
4. Blenden, D. C., Bell, J. F., Tsao, A. T. and Umoh, J. U. 1983. Immunofluorescent examination of the skin of rabies-infected animals as a means of early detection of rabies virus antigen. *J. Clin. Microbiol.* **18**: 631–636. [Medline] [CrossRef]
5. Blenden, D. C., Creech, W. and Torres-Anjel, M. J. 1986. Use of immunofluorescence examination to detect rabies virus antigen in the skin of humans with clinical encephalitis. *J. Infect. Dis.* **154**: 698–701. [Medline] [CrossRef]
6. Boonsriroj, H., Manalo, D. L., Kimitsuki, K., Shimatsu, T., Shiwa, N., Shinozaki, H., Takahashi, Y., Tanaka, N., Inoue, S. and Park, C. H. 2016. A pathological study of the salivary glands of rabid dogs in the Philippines. *J. Vet. Med. Sci.* **78**: 35–42. [Medline] [CrossRef]
7. Dimaano, E. M., Scholand, S. J., Alera, M. T. and Belandres, D. B. 2011. Clinical and epidemiological features of human rabies cases in the Philippines: a review from 1987 to 2006. *Int. J. Infect. Dis.* **15**: e495–e499. [Medline] [CrossRef]
8. Evans, H. E. 2013. Miller's Anatomy of the Dog, 4th ed., pp. 712–715. Elsevier Saunders, St. Louis.
9. Fekadu, M. and Shaddock, J. H. 1984. Peripheral distribution of virus in dogs inoculated with two strains of rabies virus. *Am. J. Vet. Res.* **45**: 724–729. [Medline]
10. Iseni, F., Barge, A., Baudin, F., Blondel, D. and Ruigrok, R. W. 1998. Characterization of rabies virus nucleocapsids and recombinant nucleocapsid-like structures. *J. Gen. Virol.* **79**: 2909–2919. [Medline] [CrossRef]
11. Jackson, A. C. 2011. Update on rabies. *Res. Rep. Trop. Med.* **2**: 31–43. [Medline]
12. Jackson, A. C. 2013. Rabies, 3rd ed., pp. 179–213. Elsevier Saunders, Philadelphia.
13. Kristensson, K., Dastur, D. K., Manghani, D. K., Tsiang, H. and Bentivoglio, M. 1996. Rabies: interactions between neurons and viruses. A review of the history of Negri inclusion bodies. *Neuropathol. Appl. Neurobiol.* **22**: 179–187. [Medline] [CrossRef]
14. Lahaye, X., Vidy, A., Pomier, C., Obiang, L., Harper, F., Gaudin, Y. and Blondel, D. 2009. Functional characterization of Negri bodies (NBs) in rabies virus-infected cells: Evidence that NBs are sites of viral transcription and replication. *J. Virol.* **83**: 7948–7958. [Medline] [CrossRef]
15. Matsumoto, S. 1962. Electron microscopy of nerve cells infected with street rabies virus. *Virology* **17**: 198–202. [Medline] [CrossRef]
16. McElhinney, L. M., Marston, D. A., Brookes, S. M. and Fooks, A. R. 2014. Effects of carcase decomposition on rabies virus infectivity and detection. *J. Virol. Methods* **207**: 110–113. [Medline] [CrossRef]
17. Moll, I., Roessler, M., Brandner, J. M., Eispert, A. C., Houdek, P. and Moll, R. 2005. Human Merkel cells--aspects of cell biology, distribution and functions. *Eur. J. Cell Biol.* **84**: 259–271. [Medline] [CrossRef]
18. Montagna, W., Roman, N. A. and Macpherson, E. 1975. Comparative study of the innervation of the facila disc of selected mammals. *J. Invest. Dermatol.* **65**: 458–465. [Medline] [CrossRef]
19. Narisawa, Y., Hashimoto, K., Nihei, Y. and Pietruk, T. 1992. Biological significance of dermal Merkel cells in development of cutaneous nerves in human fetal skin. *J. Histochem. Cytochem.* **40**: 65–71. [Medline] [CrossRef]
20. Ramírez, G. A., Rodríguez, F., Quesada, Ó., Herráez, P., Fernández, A. and Espinosa-de-Los-Monteros, A. 2016. Anatomical mapping and density of Merkel cells in skin and mucosae of the dog. *Anat. Rec. (Hoboken)* **299**: 1157–1164. [Medline] [CrossRef]
21. Shimatsu, T., Shinozaki, H., Kimitsuki, K., Shiwa, N., Manalo, D. L., Perez, R. C., Dilig, J. E., Yamada, K., Boonsriroj, H., Inoue, S. and Park, C. H. 2016. Localization of the rabies virus antigen in Merkel cells in the follicle-sinus complexes of muzzle skins of rabid dogs. *J. Virol. Methods* **237**: 40–46. [Medline] [CrossRef]
22. Shiwa, N., Kimitsuki, K., Manalo, D. L., Inoue, S. and Park, C. H. 2018. A pathological study of the tongues of rabid dogs in the Philippines. *Arch. Virol.* **163**: 1615–1621. [Medline] [CrossRef]
23. Shiwa, N., Manalo, D. L., Boldbaatar, B., Noguchi, A., Inoue, S. and Park, C. H. 2020. Follicle-sinus complexes in muzzle skin of domestic and wild animals as diagnostic material for detection of rabies. *J. Vet. Med. Sci.* **82**: 1204–1208. [Medline] [CrossRef]
24. Shiwa, N., Nakajima, C., Kimitsuki, K., Manalo, D. L., Noguchi, A., Inoue, S. and Park, C. H. 2018. Follicle sinus complexes (FSCs) in muzzle skin as postmortem diagnostic material of rabid dogs. *J. Vet. Med. Sci.* **80**: 1818–1821. [Medline] [CrossRef]
25. Tuminaite, I. and Kröger, R. H. H. 2021. Rhinarium skin structure and epidermal innervation in selected mammals. *J. Morphol.* **282**: 419–426. [Medline] [CrossRef]
26. World Health Organization. 2018. WHO expert consultation on rabies, Third report. *World Health Organ. Tech. Rep. Ser.* 1012.
27. World Organisation for Animal Health (OIE). 2018. Manual of diagnostic tests and vaccines for terrestrial animals 2019. https://www.oie.int/standardsetting/terrestrial-manual/access-online/. OIE, Paris, France [accessed on May 1, 2021].